Abstract :
Tires are made of viscoelastic materials with stiffness quite dependent on the frequency. Generally, two causes of the stiffness increase are distinguished: a frequency dependence complex modulus and a geometrical stiffness. In this paper, an experimental and theoretical study on the relaxation and frequency dependence of complex moduli of the tire constitutive materials are presented and validated. Expressions of the viscoelastic behavior are presented in time and frequency domains. The results show that the real part of the Young's modulus is monotonic according to the frequency. It contributes to an important part of the stiffening.
A numerical approach simulating the experimental results of the contact area of Cesbron is also presented. The tire is modeled with a real material distribution in the tire section. The geometrical stiffness also increases with the rotational velocity and it varies with the vibration frequencies. Static and dynamic computations for different rolling velocities are done. The results show that the contact area depends on the velocity of the rolling tire. Comparisons between the measurements and the computations show a good agrement and a decrease of about 20 % in the contact areas when the tire rolls compared to a static tire. This difference can be explained by the viscoelastic properties of the materials.

Keywords: Complex modulus, rolling tire, contact area, velocity

1 Introduction

The understanding of the tire behaviour during the rolling and of the tire noise production mechanisms are still major challenges in the field of car design. A correct modelling of these mechanisms requires a deep knowledge of parameters affecting the tire-road contact, in particular the contact area. In detail, it has been proven experimentally [1] that the contact area depends on several factors, like the tire geometry, the asperities of the road, the rolling velocity and the material distribution in the tire section.

In this paper, two factors affecting the tire-road contact area are analyzed: (i) the frequency dependence of the material constitutive properties and (ii) the rolling velocity.

The composite material constituting a tire is thought as a homogenized material, having a visco-elastic behaviour. It is supposed here that the corresponding relaxation function has the form of a standard Prony's series. In the first part of this article, the relaxation tests are presented and discussed. In particular, the complex modulus is derived from the relaxation function accounting for the influence of the initial fast loading phase preceding the true relaxation phase with constant strain. By this procedure, it is possible to get a correct expression of the complex modulus, removing the errors associated to the usual formulas based on the assumption that the constant strain of the relaxation test is applied instantaneously. The analysis of the relaxation test data obtained at the laboratory shows that the storage modulus (i.e. the real part of the complex modulus) at zero frequency is sensibly less than at frequencies of some tenth of Hertz. The dynamic tests performed with a hammer-sensor excitation-measurement system confirm this behaviour. This increment of the storage modulus for increasing frequencies shows that there is a stiffening effect associated with the material under dynamic conditions.

An experimental campaign has been realized at the LCPC (Laboratoire Central des Ponts et Chausses France), in order to evaluate the influence of rolling velocity on the tire-road contact area. For both static and rolling conditions, the contact area has been measured for a smooth/non-smooth tire on a smooth/non-smooth road. In the static load case, the tire supports only the car weight. In the other case, the contact area is calculated from pressure measurements [1]. The results show that the contact area has a tendency to converge toward an asymptotic value for increasing rolling velocity (up to 50 km/h in the available test data).

To simulate this, the tire-road contact is modeled with the finite element code ANSYS. The real geometry and material distribution of the tire are implemented. Only the case of smooth road is considered. First, a static analysis is performed with the static material properties obtained from experimental measures and the corresponding contact area is computed. Then, the rolling effect is taken into account into the tire finite element simulation. The constitutive material properties obtained from the relaxation tests are implemented and the contact area is evaluated also in this case and it proves to be smaller than in the static case. We can conclude that there is a good agreement between experimental and numerical results.

2 Relaxation and complex moduli

In principle, the viscoelastic behavior can be identified by the relaxation tension test. The viscoelasticity is presented by the characteristic times. These times have an important role in the dynamical domain. The Fourier transform shows that the complex modulus at high frequencies is mainly influenced by the smallest times. In this section, it is assumed that the relaxation modulus is expressed in a Prony's series form in which the characteristic times appear in the exponential term. Since the initial time is not zero, an identification technique with the non-zero time is presented. The real stress is analytically expressed via the Prony's series terms. The coefficients respective to the exponential form are determinated by Curve Fitting Toolbox in Matlab. Hence,

the relaxation modulus is specified.

The rubber takes a major part in the material distribution of the tire section. Though, the tread belt layer supports the most of the static stresses occurring in the tire. The Fig. 1 presents the constitutive materials in the tire section and the tread belt macro layer which is composed by two elementary layers with the parallel wires and a rubber layer. In particular the mechanical properties this layer are studied in the next part of this paper.

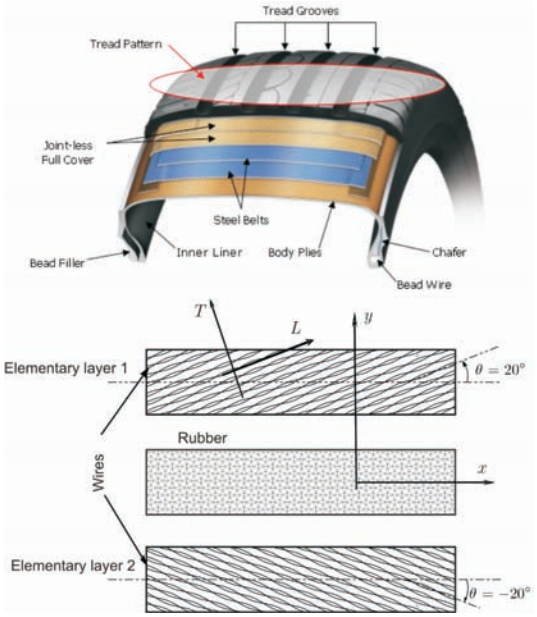

Figure 1: Composition of a tire and of the tread belt macro layer

2.1 Relaxation modulus and relaxation stress

The relaxation stress can be expressed by a Stieltjes integral [3, 2],:

$$\sigma_{ij}(t) = \int_0^t R_{ijkl}(t-\tau)\frac{\partial \varepsilon_{kl}(\tau)}{\partial \tau}d\tau + R_{ijkl}(t)\varepsilon(0)$$

$$= R_{ijkl}(0)\varepsilon(t) + \int_0^t \frac{\partial R_{ijkl}(\tau)}{\partial \tau}\,\varepsilon_{kl}(t-\tau)d\tau \quad (1)$$

or by the tensor form:

$$\boldsymbol{\sigma}(t) = \boldsymbol{R}(t) * \frac{D\boldsymbol{\varepsilon}}{D\tau} \quad (2)$$

where $\boldsymbol{R}(t)$ is the relaxation modulus tensor of degree 4, $\frac{D\boldsymbol{\varepsilon}}{D\tau}$ is the distribution derivation (includes the discontinuity in time). The relaxation function is presented by the Prony's series:

$$R(t) = A_0 + \sum_{i=1}^{N} A_i e^{-\frac{t}{\tau_i}} \quad (3)$$

In practice, an instantaneous strain can be not carried out $\varepsilon(t) = H(t)\varepsilon_0$ at the instant $t = 0$ (H(t) is the Heaviside function). Thus, the strain is supposed to reach the maximal value ε_0 in the interval $[0, t_0]$ by a linear variation of $\varepsilon(t)$. This quantity is analytically expressed (Fig. 2):

$$\varepsilon(t) = \varepsilon_0 \left[H(t-t_0) + \frac{t}{t_0}\left(H(t) - H(t-t_0)\right)\right] \quad (4)$$

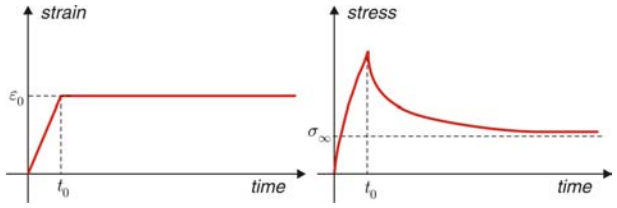

Figure 2: Real time relaxation strain and stress

The viscoelastic behaviour is established in two cases:

- $0 \leq t < t_0$:

Assuming that in the interval $[0, t_0]$, the strain varies linearly, $\varepsilon(t) = t\frac{\varepsilon_0}{t_0}$, we obtain:

$$\sigma(t) = \frac{\varepsilon_0}{t_0}\int_0^t R(t-\tau)d\tau = \frac{\varepsilon_0}{t_0}\int_0^t R(\tau)d\tau \quad (5)$$

- $t_0 \leq t$:

The derivative of the strain in the interval $[t_0, t]$ is cancelled.

$$\sigma(t) = \int_0^t R(t-\tau)\frac{\partial \varepsilon(\tau)}{\partial \tau}d\tau = \frac{\varepsilon_0}{t_0}\int_0^{t_0} R(t-\tau)d\tau \quad (6)$$

Hence, the relaxation stress is deduced in term of the characteristic times and the associated magnitudes :

$$\sigma(t) = \frac{\varepsilon_0}{t_0}\left[H(t-t_0)\left(\sum_{i=1}^{N} A_i\tau_i\left(e^{\frac{t_0-t}{\tau_i}} - 1\right) - A_0(t-t_0)\right)\right.$$

$$\left. -H(t)\left(\sum_{i=1}^{N} A_i\tau_i\left(e^{\frac{-t}{\tau_i}} - 1\right) - A_0 t\right)\right] \quad (7)$$

Knowing that the exponential function is a convex base, the stress relaxation can be identified only where the convexity is ensured. In this case, the studied time is divided in two intervals: before and after the instant t_0. In each interval, the stress is convex but it is not convex in the whole time. The free coefficient A_0 is the elastic modulus and the interval $[t_0, T_{max}]$ is chosen for the identification. The stress is depicted as below:

$$\sigma(t) = \frac{\varepsilon_0}{t_0}\left[A_0 t_0 + \sum_{i=1}^{N} A_i\tau_i e^{-\frac{t}{\tau_i}}\left(e^{\frac{t_0}{\tau_i}} - 1\right)\right] \quad (8)$$

The Curve Fitting Toolbox in Matlab is used to identify the parameters. The fitting consists in minimizing the error function, which is the difference between the measured and estimated values. The number of exponential terms is chosen as small as possible. The value N is increased until the best solution is found. Its is noted that a bigger N does signify a better solution because the minimization algorithm can conduct to a local minimum. Another control is to limit the elastic modulus A_0 to reach a good fit at the end of the curve.

The elementary layer is supposed to be composed of the parallel wires and the rubber. The macro layer of the tread belt is composed of two elementary layers and a rubber layer at the middle (Fig. 1). The thickness of each layer is 0.6mm. This macro layer supports the highest circumferential tension stress in the tire. However, it takes the role to keep a good contact road-tire and to protect the tire. This layer is mainly studied.

The result of the modulus identification by the relaxation stress is presented in the Fig. 3 and in the Tab. 1 and 2.

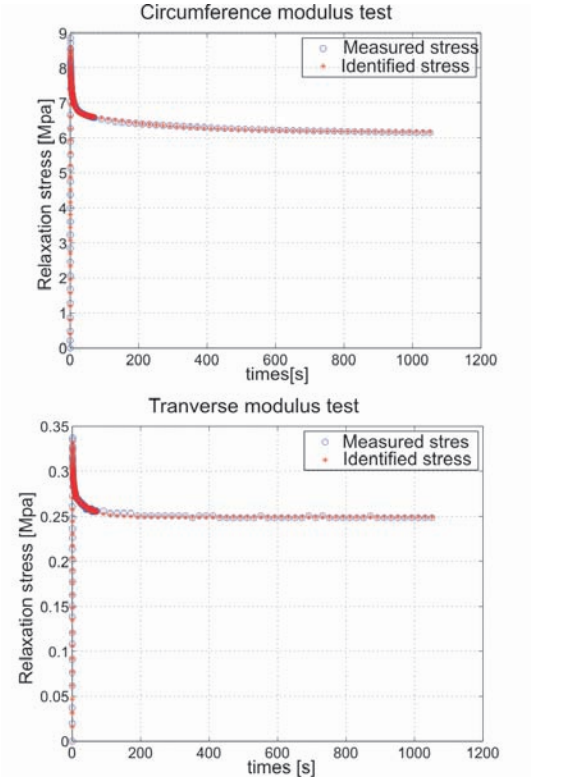

Figure 3: Relaxation stress identification for the moduli in the two main tire directions

	A_0	A_1	A_2	A_3
E_x	356.5974	34.1506	59.7337	139.8615
E_y	9.9238	1.2488	6.0636	3.1896

Table 1: Term coefficients of tests in the two main directions

	t_0	t_1	t_2	t_3
E_x	1.2000	212.2070	7.3106	0.5625
E_y	1.2000	46.7811	4.2929	0.5652

Table 2: Initial and characteristic times of tests in the two main directions

2.2 Complex modulus

The complex modulus depends on the frequency because of the viscoelasticity. In the same way, the relaxation modulus of the elementary layer is measured. All the moduli tested can be expressed analytically in the Prony's series form. With a homogenization process for a multi-layer composite, the apparent modulus of the macro layer can be calculated from the data of the elementary layers.

In the other way, the Fourier transform from the time domain into the frequency domain gives us the analytical expression of the macro layer in term of the frequency. Finally, the direct measurement of the complex modulus by the beam vibration formula is used. The FRF (Frequency Response Function) is measured by the Bruel & Kjaer sensors. These signals are treated by the software PulseLabShop. Analytically, the eigenfrequencies are expressed as [4]:

$$f_n = \frac{(\beta_n l)^2}{2\pi l^2}\sqrt{\frac{EI}{\rho A}} \tag{9}$$

where $\beta_n l$ is the wave number on the beam length. In the clamped-free case, it satisfies the equation:

$$\cos(\beta_n l)\cosh(\beta_n l) + 1 \quad = \quad 0 \tag{10}$$

The measured eigenfrequencies give the real part of the complex modulus. The damping ratio detected by PulseLabShop gives the imaginary one. The calculated and measured apparent moduli are showed in the Figs. 4 and 5.

3 Tire-road contact area test

The contact test has been realized by Cesbron. This author did an experimental and numerical study on the multi-asperity contact. However, in this paper, only the contact test results of the smooth tire with a plane foundation is used to compare with the numerical one.

3.1 Contact measurement method

The area and the contact pressure can be measured with the help of the sensors disposed at the interface of two solids. There are two sensors categories: the film which is sensible to the contact pressure post-processed by an image treatment and the real time pressure acquisition cells. With the rolling tire case, the pressure is measured by the Tekscan 3150 cells . The description of this equipment is shown in the Fig. 6. The measurement is realized on a real vehicle (Renault Scenic, 2.0L/16V). This vehicle is equipped of two standard front tires and two smooth back tires. These two smooth tires are competition tires. The contact pressure on the right back tire is measured. The other tires are placed at the same level to ensure the identical forces on four tires. The vehicle body is elevated on the contact level and positioned with precision to apply the tire load on the contact plate.

According to the constructor, the stiffness of the used competition tire is of the same order as the standard

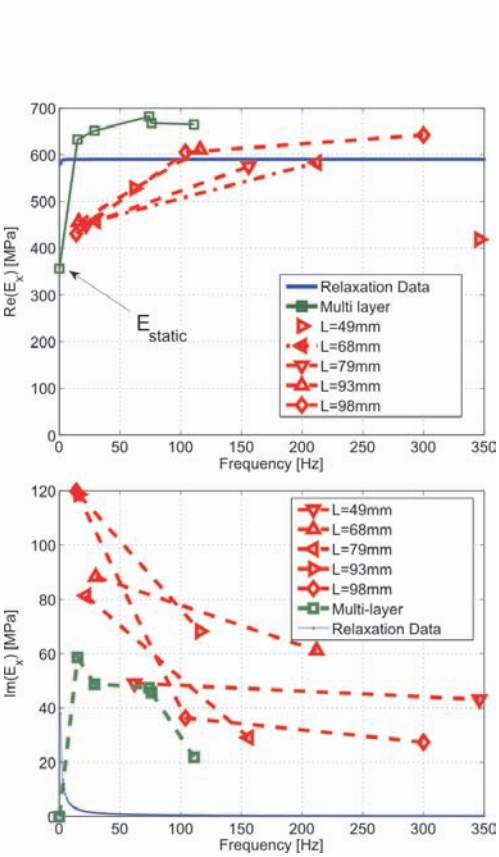

Figure 4: Circumferential apparent modulus comparison of the macro layer exploited from the relaxation data, calculated by the homogenization process and in several beam lengths

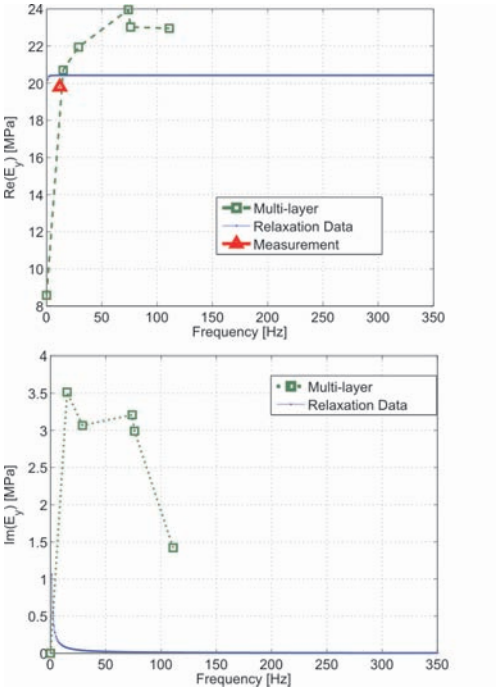

Figure 5: Transverse apparent modulus comparison of the macro layer exploited from the relaxation data and calculated by the homogenization process

ones. Finally, the pumping pressure is 0.22 MPa (2.2 bars) and this value is controlled before each test.

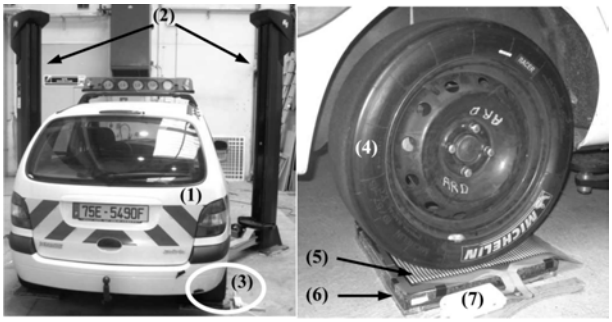

Figure 6: Experimental disposition of the contact test: 1.Test vehicle 2.Lifting bridge 3.Studied contact zone 4.Smooth tire 5.Tekscan sensor 6.Reference plate 7.Tekscan box [1]

3.2 Test result

At a moment, each cell gives a contact pressure in term of time. The real time pressure reconstruction of all the cells gives us the contact pressure distribution of the studied zone. The contact area is measured in several cases of road asperity (Fig. 7). It is calculated by the formula:

$$A = V \int_{t_1}^{t_2} L(t)dt \tag{11}$$

where V is the vehicle velocity and $L(t)$ is the contact length measured at each instant, t_1, t_2 are the beginning and final contact times.

The result is presented in the Fig. 8 and the Tab. 3.

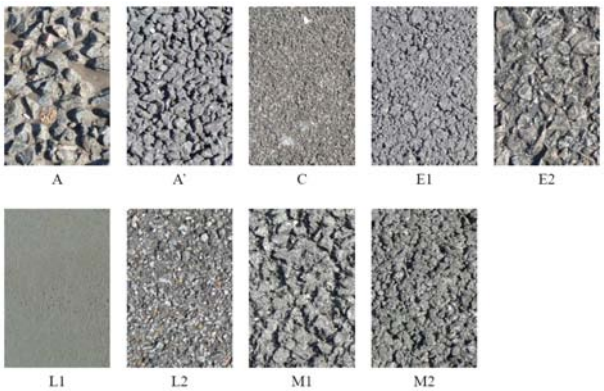

Figure 7: Tested road surface [1]

4 Tire modeling and comparison with the experiments

4.1 Geometry and load applied

In this paper, the tire modeling is realized with the smooth tire. The section geometry is measured from a real section. A revolution process generates the whole of the model. The wheel is modeled as the fixed boundary condition. The road is supposed smooth and modeled by a plate. The contact is therefore between two smooth surfaces. The model is presented in the Fig. 9.

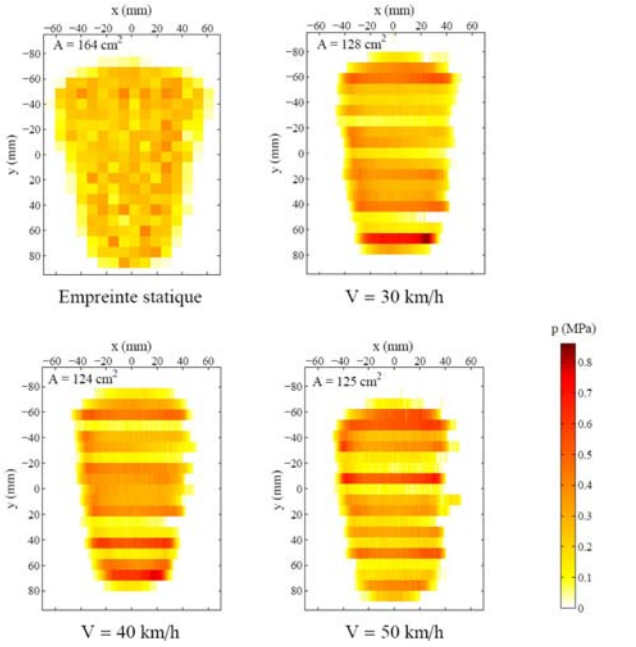

Figure 8: Contact area in the static case and for the 3 different velocities considered [1]

Road surface	Static	30km/h	40km/h	50km/h
A'	156	123	123	122
C	155	130	129	123
E1	164	128	124	125
E2	151	133	137	131
M2	151	134	131	136
L1	148	121	126	122
L2	160	122	122	121

Table 3: Evolution of contact area in term of the velocity [1]

The applied force on the tire is replaced by the pressure in the plate. The tested force is $F = 3300N$ giving a pressure

$$p = \frac{F}{a^2} = \frac{3300}{0.4^2} = 20625N/m^2 \qquad (12)$$

where a is the length size of the square plate. The tire is fixed on the wheel. To stabilize the model, we fix some nodes of the plate in the horizontal displacement. The inner pressure is taken equal to 2.2 bars.

The finite element software ANSYS is used to solve this problem. The rolling velocity is introduced by the rotating angular velocity $\Omega = \frac{V}{R_{tire}}$. First, we introduce the static moduli into the model to calculate the contact area in the static case. The contact area includes the zones where the pressure contact or the stress intensity is considered as large enough.

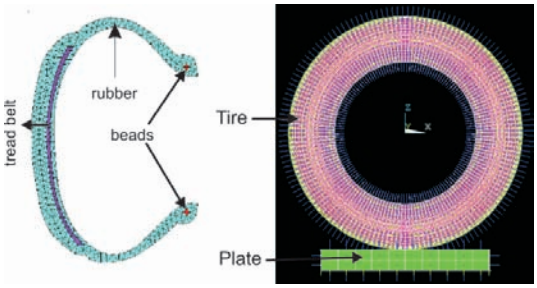

Figure 9: Modeling of the road-tire contact in ANSYS

4.2 Result and comparison

The result is saved in graphic form (Fig. 10). The contact area is determinated by the connected elements on the two contact sides (Fig. 12). The results show a good agrement with the measurement.

Figure 10: Vertical static stress in the road-tire contact problem

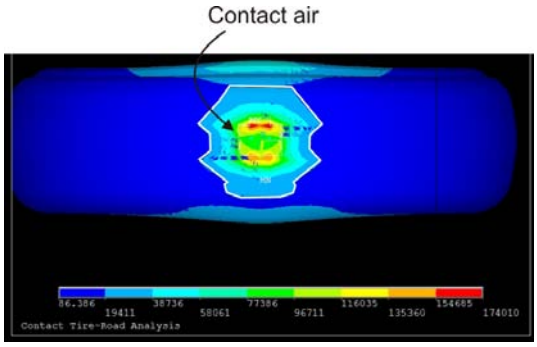

Figure 11: Stress intensity and calculated contact area

5 Conclusion

An identification technique of the relaxation stress is presented in this paper. The analytical expressions of the relaxation modulus are deduced. The Fourier transform gives the dependence of complex moduli with the frequency. An homogenization process is done to calculate the apparent moduli of the macro layer. The vibration test gives the equivalent dynamical moduli and confirms the stiffening of the materials when the frequency is increased.

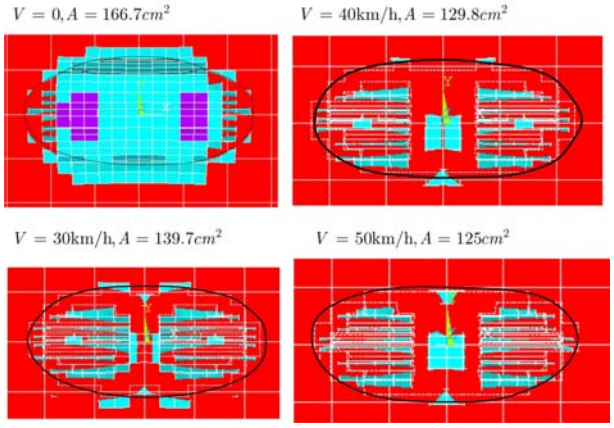

Figure 12: Road-tire contact areas calculated by ANSYS

A road-tire contact test is realized in the frame of the Cesbron's thesis [1]. The test shows that when the velocity varies, the contact area varies too. However, there is a coupling between the velocity dependence and the dependence with the frequency of the complex modulus and it is the cause of the variation of the contact area.

When the vehicle moves,the tire rotates and the materials work at different frequencies. As the rigidity of the materials is quite different in rotation and in dynamics, this explains the reduction in contact area as the tire rolls.

References

[1] J. Cesbron, "Influence de la texture de chausse sur le bruit de contact pneumatique/chausses", *PhD Thesis-Ecole Central de Nantes*, (2007)

[2] J. Lemaitre and J.-L. Chaboche, "Mcanique des matriaux solides", *Dunod*, (2004)

[3] Y. Chevalier, "Comportements lastique et viscolastique des composites", *Techniques de l'Ingnieur, trait Plastiques et Composites - Vol ARCH1*, (1988)

[4] J. Courbon, "Vibrations des poutres", *Techniques de l'Ingnieur - trait Construction*, (1984)